Phenylalanine 90 and 93 Are Localized within the Phenol Binding Site of Human UDP-Glucuronosyltransferase 1A10 as Determined by Photoaffinity Labeling, Mass Spectrometry, and Site-...

ARTICLE *in* BIOCHEMISTRY · MARCH 2006

Impact Factor: 3.02 · DOI: 10.1021/bi0519001 · Source: PubMed

8 AUTHORS, INCLUDING:

Stacie M. Bratton
University of Arkansas for Medical Sciences
34 PUBLICATIONS **602** CITATIONS
SEE PROFILE

Eric Battaglia
University of Lorraine
36 PUBLICATIONS **946** CITATIONS
SEE PROFILE

Anna Radominska-Pandya
University of Arkansas for Medical Sciences
186 PUBLICATIONS **5,525** CITATIONS
SEE PROFILE

Phenylalanine 90 and 93 Are Localized within the Phenol Binding Site of Human UDP-Glucuronosyltransferase 1A10 as Determined by Photoaffinity Labeling, Mass Spectrometry, and Site-Directed Mutagenesis†

Yan Xiong,‡ Dan Bernardi,§ Stacie Bratton,‡ Michael D. Ward,|| Eric Battaglia,§ Moshe Finel,⊥ Richard R. Drake,|| and Anna Radominska-Pandya*,‡

Department of Biochemistry and Molecular Biology, University of Arkansas for Medical Sciences, Little Rock, Arkansas 72205, LIMBP, Paul Verlaine University, Metz, France, Center for Biomedical Proteomics, Department of Microbiology and Molecular Cell Biology, Eastern Virginia Medical School, Norfolk, Virginia 23507, and Viikki DDTC, Faculty of Pharmacy, University of Helsinki, Helsinki, Finland

Received September 16, 2005; Revised Manuscript Received December 12, 2005

ABSTRACT: 4-Azido-2-hydroxybenzoic acid (4-AzHBA), a novel photoactive benzoic acid derivative, has been synthesized and used as a photoprobe to identify the phenol binding site of UDP-glucuronosyltransferases (UGTs). Analysis of recombinant His-tag UGTs from the 1A family for their ability to glucuronidate *p*-nitrophenol (pNP) and 4-methylumbelliferone (4-MU) revealed that UGT1A10 shows high activity toward phenols and phenol derivatives. Purified UGT1A10 was photolabeled with 4-AzHBA, digested with trypsin, and analyzed by matrix-assisted laser desorption/ionization time-of-flight (MALDI-TOF)-mass spectrometry. A single modified peak corresponding to amino acid residues 89−98 (EFMVFHAQWK) of UGT1A10 was identified. The attachment site of the 4-AzHBA probe was localized to the quadruplet Phe^{90}-Met^{91}-Val^{92}-Phe^{93} using ESI LC−MS/MS. Sequence alignment revealed that the Phe^{90} and Phe^{93} are conserved in UGT1A7−10. Site-directed mutagenesis of these two amino acids was then followed by kinetic analysis of the mutants with two phenolic substrates, pNP and 4-MU, containing one and two planar rings, respectively. Using the combination of photoaffinity labeling, enzymatic digestion, MALDI-TOF and LC-MS mass spectrometry, and site-directed mutagenesis, we have determined for the first time that Phe^{90} and Phe^{93} are directly involved in the catalytic activity of UGT1A10 toward 4-MU and pNP.

UDP-glucuronosyltransferases (UGTs[1]) are a family of membrane glycoproteins located in the endoplasmic reticulum (ER). These enzymes are synthesized as precursors of about 530 residues containing a N-terminal signal peptide that mediates the integration of the polypeptide chain into the ER (*1*−*3*). The mature protein of about 505 residues is classified as a type I ER transmembrane protein (*4*) with a lumenal domain consisting of about 95% of the polypeptide chain and a cytoplasmic domain of only 20 or so residues (*5*, *6*). Based on protein sequence homology analysis of UGT1A isoforms, it has been generally postulated that the conserved C-terminal domain binds the cosubstrate, UDP-glucuronic acid (UDP-GlcUA), whereas the variable N-terminal domain binds substrates and determines the substrate specificity. Specifically, the most variable amino acids are located between amino acid residues 55−180. Information on the subcellular localization of UGTs with special emphasis on the association of this protein with the ER, as well as the structural determinants of UGTs in relation to membrane association, residency, and enzymatic activity has developed recently due to data obtained by molecular modeling, bioinformatics tools such as sequence alignment, and comparison with selected crystallized glycosyltransferases (*7*). However, progress in the identification of UGT-binding sites remains undeveloped.

UGTs are of particular physiological, pharmacological, and toxicological significance due to their involvement in the biotransformation of the largest number of endogenous compounds, drugs, and environmental toxins of different chemical structures and origins of any phase II metabolizing enzyme (*8*). There is a tremendous need for an understanding of the pharmacogenetics and drug interactions of compounds that are substrates for and/or inducers of UGTs. However, the rigorous structural studies of UGTs and their active sites necessary to understand the mechanistic aspects of UGT substrate specificity, inhibition, and drug-drug interactions have been hampered by a lack of purified protein. This lack

† This work was supported in part by the NIH Grants DK51971, DK49715 (A.R.-P.), and CA908028 (R.R.D.), Tobacco Settlement Funds (A.R.-P.), and the Academy of Finland, Project 207535 (M.F.).

* Corresponding author. Telephone: 501-686-5414. Fax: 501-603-1146. Email: RadominskaAnna@uams.edu.

‡ University of Arkansas for Medical Sciences.

§ Paul Verlaine University.

|| Eastern Virginia Medical School.

⊥ University of Helsinki.

[1] Abbreviations: 2-AzBA, 2-azidobenzoic acid; 2-AzNBA, 2-azido-4-nitrobenzoic acid; 3-AzBA, 3-azidobenzoic acid; 3-AzCBA, 2-azido-4-chlorobenzoic acid; 4-AzBA, 4-azidobenzoic acid; 4-AzHBA, 4-azido-2-hydroxybenzoic acid; 4-MU, 4-methylumbelliferone; AzMC, 7-azido-4-methylcoumarin; ER, endoplasmic reticulum; IMAC, immobilized metal affinity chromatography; MALDI-TOF, matrix-assisted laser desorption/ionization time-of-flight-mass spectrometry; pNP, para-nitrophenol; UDP-GlcUA, UDP-glucuronic acid; UGT, UDP-glucuronosyltransferase.

10.1021/bi0519001 CCC: $33.50
Published on Web 01/27/2006

of structural knowledge has resulted in the prediction of UGT binding site structures by utilizing selective inhibitors, amino acid-specific chemical modification reagents, and amino acid alignments (*9*−*15*). There are only a few reports of computer-aided molecular modeling being applied to this system (*14*, *16*), and site-directed mutagenesis studies are limited (*13*, *17*−*20*).

Photoaffinity labeling is an important approach to the identification of crucial amino acids in the active site of enzymes and transporters. This method is especially useful for mapping active sites of proteins in the absence of known tertiary structures (*21*). Compared with other methods, photolabeling has the advantage of providing direct evidence for spatial approximations between the site of covalent labeling and the residue that was modified by the photoaffinity probe. It is the most direct and unambiguous method for determining the binding-site architecture of enzymes.

Our laboratory has carried out photoaffinity labeling experiments with several protein types, such as UGTs, sulfotransferases (*22*, *23*), RA binding proteins (*24*, *25*), protein kinase C (*26*), and the nuclear receptor RXR (*27*). Our labeling studies of the UGT substrate binding sites were based on the development of novel photoaffinity probes directed toward both the aglycon and UDP-GlcUA binding sites (*9*, *28*−*35*). One such probe, 7-azido-4-methylcoumarin (AzMC), a fluorescent photoactive analogue of the UGT1A6 marker substrate 4-MU, was synthesized and used to specifically label the substrate binding site of human recombinant UGT1A6 (*28*). That study showed that AzMC was specifically directed toward the substrate binding site of UGT1A6 and was suitable for use in the identification of amino acids in the substrate binding sites. However, due to the lack of purified UGT protein, we were prohibited from identifying the specific amino acids involved in the binding of the photoaffinity probe. In the present studies, the availability of large amounts of purified UGT protein expressed with a N-terminal His-tag in baculovirus infected Sf9 insect cells (*36*) has allowed us to identify the exact location of the photolabeled amino acids by LC−MS/MS sequencing.

The first His-tagged recombinant UGT isoform to be used in the present photoaffinity labeling studies is UGT1A10. UGT1A10 is highly expressed in numerous target tissues such as the gastrointestinal tract (*37*−*39*) and the upper aerodigestive tract (*40*). The broad tissue distribution and substrate specificity of UGT1A10 indicate that it may contribute to the extrahepatic detoxification of endogenous and xenobiotic compounds, especially orally administered drugs and food-borne/environmental carcinogens. Although there are many studies focused on the substrate specificity of UGT1A10, studies attempting to identify catalytically important amino acids are few (*41*, *42*). Recent studies of UGT1A10 substrate specificity showed that this isoform accepts a variety of exogenous and endogenous compounds that contain several key structural similarities. These include both single and multiple aromatic ring systems containing a variety of ring substitutions, such as hydroxyl and carboxyl groups as well as chlorines and amines. The most important substrates toward which UGT1A10 exhibits glucuronidation activity are as follows: simple phenols (*43*), estrogens (*44*), androgens (*44*), flavonoids (*45*), fatty acids (*46*), metabolites of benzo[*a*]pyrene (a carcinogen found in tobacco smoke) (*47*), and 2-hydroxyamino-1-methyl-6-phenylimidazo-(4,5-*b*) pyridine (a heterocyclic amine found in overcooked food) (*9*, *47*−*51*).

To elucidate the structural basis for UGT1A10 substrate specificity at the molecular level and obtain a better understanding of the mechanism of glucuronidation, we used the newly synthesized photoactive azidobenzoic acid derivatives to photolabel human recombinant UGT1A10. Enzymatic studies of UGT1A10 with the azidobenzoic acid derivatives identified four compounds that were accepted as substrates by UGT1A10 and, thus, are probable photolabeling probes that can be used to identify the phenol binding site of UGT1A10. One of these compounds, 4-azido-2-hydroxybenzoic acid (4-AzHBA), was selected for initial experiments to identify the phenol binding site of UGT1A10. Using homogeneous UGT1A10 protein and this phenol-related photoaffinity probe, we observed efficient photocrosslinking of 4-AzHBA to the highly hydrophobic "patch" created by Phe^{90}-Met^{91}-Val^{92}-Phe^{93} in the N-terminal region of UGT1A10. We postulate that this "patch", specifically the aromatic side chains of Phe^{90} and Phe^{93}, interacts with the phenolic substrates through ring stacking. Site-directed mutagenesis of Phe^{90} and Phe^{93} supported the prediction that a phenol binding site of UGT1A10 lies within the N-terminal end in the region of residues 90−93.

EXPERIMENTAL PROCEDURES

Materials. [^{14}C]4-Nitrophenol (pNP; 6.4 mCi/mmol), 4-MU, saccharolactone (saccharic acid-1,4-lactone), UDP-GlcUA and horseradish peroxidase-conjugated mouse anti-rabbit IgG were purchased from Sigma Chemical Co. (St. Louis, MO). [^{14}C]UDP-GlcUA ([^{14}C]UDPGlcUA; sp. act.: 325 mCi/mmol) was purchased from PerkinElmer Life Sciences (Boston, MA). Triton X-100 was obtained from Fisher Scientific (Pittsburgh, PA). The His Hi-trap columns and ECL Western blotting detection system were purchased from Amersham Bioscience (Piscatway, NJ). Anti-UGT1A antibody was from BD BioSciences (San Jose, CA). All other chemicals and solvents were of analytical grade.

Synthesis of a Series of Azido Derivatives of Benzoic Acid. 4-Azido-2-hydroxybenzoic acid (4-AzHBA) and five other azido derivatives of benzoic acid were synthesized. Briefly, the synthesis was carried out by reacting the amino moiety of the appropriate amino benzoic acid dissolved in sulfuric acid and treated with $NaNO_2$ yielding the corresponding diazonium salt, which was then reacted with NaN_3 to yield an azido product. All six azidobenzoic acids (structures shown in Figure 1) were prepared in the same way.

2-Azidobenzoic Acid (2-AzBA). Beige solid; Yield = 75%; mp = 146−148 °C; ^{1}H NMR ($CDCl_3$): δ_H = 8.17−8.13 (d, J = 9.5 Hz, 1H), 7.65−7.59 (t, 1H), 7.51−7.44 (t, 1H), 7.30−7.24 (m, 2H); IR (neat): ν = 2101 (N_3), 1687−1668 (C═O), 1250 cm^{-1}.

3-Azidobenzoic Acid (3-AzBA). White solid; Yield = 77%; mp = 163−165 °C; ^{1}H NMR ($CDCl_3$): δ_H = 7.90−7.87 (d, J = 7.75 Hz, 1H), 7.78 (s, 1H), 7.51−7.44 (t, J = 5.2 Hz, 1H), 7.28−7.24 (d, J = 10.25 Hz, 1H); IR (neat): ν = 2129 (N_3), 1690 (C═O), 1300 cm^{-1}.

4-Azidobenzoic Acid (4-AzBA). White solid; Yield = 75%; mp = 188−191 °C; ^{1}H NMR ($CDCl_3$): δ_H = 8.12−8.09 (d, J = 8.5 Hz, 2H), 7.12−7.09 (d, J = 8.5 Hz, 2H); IR (neat): ν = 2132 (N_3), 1673 (C═O), 1599, 1281 cm^{-1}.

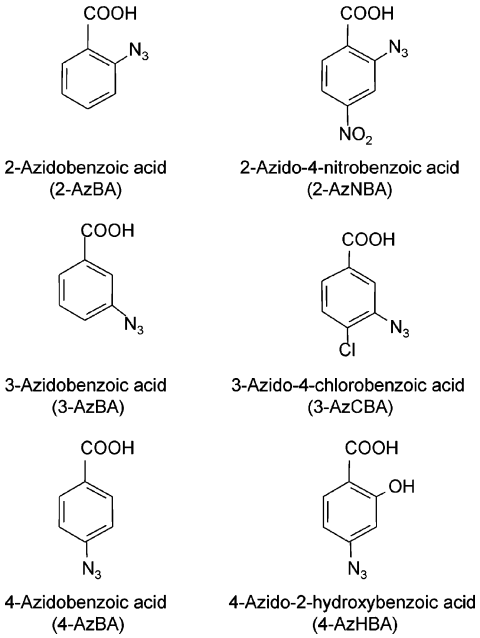

FIGURE 1: Structures of azido-benzoic acid photoaffinity probes used in these studies.

2-Azido-4-nitrobenzoic Acid (2-AzNBA). Orange solid; Yield = 50%; mp = 160 °C; R_f = 0.11 (AcOEt−cyclohexane, 1/1, v/v); ^{1}H NMR ($CDCl_3$): δ_H = 8.02−7.99 (m, 2H), 7.95−7.91 (d, J = 10,25 Hz, 1H).

3-Azido-4-chlorobenzoic Acid (3-AzCBA). White solid; Yield = 87%; mp = 194−197 °C; R_f = 0.36 (CH_2Cl_2/MeOH, 1/24, v/v); ^{1}H NMR ($CDCl_3$): δ_H = 7.82 (s, 1H), 7.70−7.67 (d, 1H), 7.38−7.35 (d, 1H); IR (neat): ν = 3600−2300 (br, OH), 2100 (N_3), 1680 cm^{-1} (C=O).

4-Azido-2-hydroxylbenzoic Acid (4-AzHBA; 4-Azidosalicylic Acid). Brownish solid; Yield = 85%; mp = 167−168 °C; ^{1}H NMR ($CDCl_3$): δ_H = 7.88 (d, J = 8 Hz, 1H), 6.59 (d, J = 8 Hz, 1H), 6.57 (s, 1H).

Cloning and Expression of Human Recombinant His-Tagged UGTs. Details of the cloning and expression of UGT1A1, 1A3, 1A4, 1A6, 1A7, 1A8, 1A9, and 1A10 in baculovirus-infected Sf9 insect cells as His-tagged proteins and the preparation of enriched membrane fractions were reported previously (*36*, *52*).

Enzymatic Assays and Kinetic Analysis. Glucuronidation of pNP was measured using previously published procedures (*28*). Briefly, for activity toward pNP, 4-MU, and the benzoic acid probes, UGT1A10 membrane protein (10 μg) was incubated in 100 mM Tris-HCl (pH 7.4)/5 mM $MgCl_2$/5 mM saccharolactone with [^{14}C]pNP (for screening) and cold pNP (25−5000 μM; for kinetic experiments), 4-MU (100−1000 μM) or benzoic acid derivative (25−2000 μM), in a total volume of 60 μL. Assays for 4-MU and the six benzoic acid derivatives were carried out under yellow light, and these substrates were dissolved in DMSO (maximum final concentration 2%). The reactions were started by the addition of either cold or [^{14}C]UDP-GlcUA (4 mM) and incubated at 37 °C for 20 min. The reaction was stopped by addition of 20 μL of ethanol.

Aliquots (60 μL) of each sample were then applied to the preabsorbent layer of channeled silica gel TLC plates (Baker 250Si-PA (19C); VWR Scientific, Sugarland, TX), and glucuronidated products and unreacted substrate were separated by development in chloroform−methanol−glacial acetic acid−water (65:25:2:4, v/v). Radioactive compounds were localized on TLC plates by autoradiography for 3−4 days at −80 °C. Silica gel in areas corresponding to the glucuronide bands identified from autoradiograms and the corresponding areas from control lanes were scraped from the TLC plate into scintillation vials, and the radioactivity was measured by liquid scintillation counting (Packard TRI-CARB 2100TR, Perkin-Elmer). The results of these experiments were analyzed, and apparent kinetic parameters were determined using Prism 4 software (GraphPad, San Diego, CA).

Inhibition of UGT1A10 Catalyzed Glucuronidation of 4-Nitrophenol (pNP) by 4-Azido-2-hydroxybenzoic Acid (4-AzHBA) in the Absence and Presence of UV Light. Experiments examining the inhibition of [^{14}C]pNP glucuronidation by 4-AzHBA in the absence and presence of UV light were performed at 37 °C. To evaluate the inhibitory potency of 4-AzHBA toward pNP glucuronidation by UGT1A10, membrane fractions enriched in UGT1A10 (10 μg) were incubated with varying concentrations of 4-AzHBA in 100 mM Tris-HCl, 5 mM $MgCl_2$, pH 7.4, for 2 min in the absence of UV irradiation. Next, [^{14}C]pNP (1 mM) was added, and reactions were started by the addition of UDP-GlcUA (4 mM). After incubation for 30 min at 37 °C in the dark, samples were analyzed by TLC and autoradiography as described above.

Protein Solubilization and Purification. The solubilization and purification of UGT1A10 were modified from the method of Kurkela et al. (*36*). Briefly, membranes were suspended in extraction medium (25 mM Tris, pH 7.5, 500 mM NaCl, 2% Triton X-100) at about 2 mg of protein/mL. The suspension was mixed for 16 h at 4 °C and then centrifuged at 41,000 × g for 1.5 h. The resultant supernatant was filtered through a 0.45-μm syringe filter to remove any particles, and the filtrate was loaded onto a nickel-charged His Hi-trap column that had been pre-equilibrated with Buffer A (25 mM Tris, pH 7.5, 500 mM NaCl, 0.05% Triton X-100, 10 mM imidazole). After extensive washing, the bound protein was eluted with a stepwise imidazole gradient, 50−400 mM, in the presence of NaCl and Triton X-100. Fractions of 1 mL were collected throughout and subjected to SDS-polyacrylamide electrophoresis (SDS-PAGE) on 10% gels, followed by either Coomassie blue staining or Western blot analysis.

Photoaffinity Labeling of Microsomal and Purified UGT1A10 with 4-Azido-2-hydroxybenzoic Acid (4-AzHBA). The optimal conditions for labeling with the novel 4-AzHBA probe were established by comparison of the effectiveness of photoaffinity labeling at two different wavelengths under slightly different conditions. Briefly, purified UGT1A10 (10 μg) was incubated with 500 μM 4-AzHBA in a total volume of 100 μL. After incubation in the dark for 1 min at 25 °C, the reaction mixture was exposed to 1) 254 nm UV light on ice for 90 s, or 2) 365 nm UV light on ice for 30 min. Each sample was subjected to this process twice to enhance the level of labeling. Both conditions were found to be highly effective; therefore, the first conditions with a shorter irradiation time and 254 nm UV light were selected for the final experiments. The reaction was stopped with 50 μL of 20% TCA and centrifuged. The protein pellet was then washed with ice cold water and resuspended in buffer (180 mM Tris (pH 7.4)/28 mM $MgCl_2$).

Proteolytic Digestion of Photolabeled UGT1A10. Photolabeled and control-irradiated UGT1A10 samples were resuspended in 50 mM NH_4HCO_3 containing 12.5 ng/μL sequencing-grade trypsin (Promega) and incubated overnight at 37 °C. The digest was desalted using PepClean C18 spin columns (Pierce Biotechnology, Rockford, IL), dried in a SpeedVac, and resuspended in 20 μL of 5% acetonitrile, 0.1% formic acid, and 0.005% heptafluorobutyric acid (HFPA) (Buffer A).

Matrix-Assisted Laser Desorption/Ionization Time-of-Flight Mass Spectrometry (MALDI-TOF). For mass spectrometry, a Bruker Daltonics UltraFlex MALDI-TOF/TOF (*53*) was used to monitor the mass spectra of tryptic digests of control and photolabeled UGTs. The UltraFlex employs ion potential lift (LIFT) (*54*) in a MALDI-TOF/TOF platform for highly sensitive (attomolar) and accurate tandem MS for peptide mass fingerprint (PMF) determinations. Lists of the obtained peptide masses were used to search protein sequence databases (MASCOT) (*55*) mediated by the Bruker BioTools software package.

LC−MS/MS. Protein digests were loaded onto a 12 cm × 0.075 mm fused silica capillary column packed with 5 μm diameter C-18 beads using a N_2 pressure vessel at 1100 psi. Peptides were eluted by applying a 55 min, 0−80% linear gradient of Buffer B (95% acetonitrile, 0.1% formic acid, 0.005% HFBA) at a flow rate of 130 μL/min with a precolumn flow splitter resulting in a final flow rate of ∼200 nL/min directly into the source. The LCQ was run in automatic collection mode with an instrument method composed of a single segment and four data-dependent scan events with a full MS scan followed by three MS/MS scans of the highest intensity peptides. Normalized collision energy was set at 30, activation Q was 0.250 with a minimum full scan signal intensity at 5×10^5 and a minimum MS2 intensity at 1×104. Dynamic exclusion was turned on utilizing a 3 min repeat count of 2 with the mass width set at 1.50 Da. The TurboSEQUEST software provided by ThermoFinnigan automatically sorted and cross-correlated the peptides in the MS/MS profile to genomic and protein database information, thus providing the protein identity.

Site-Directed Mutagenesis and Expression of Mutated Recombinant Proteins. Site-directed mutagenesis was performed using the QuickChange Site-directed Mutagenesis Kit (Stratagene, La Jolla, CA) according to manufacturer's instructions. The mutagenic primers used, with the mutated nucleotides underlined were: F90A-for: 5′-ATCAGAACCGGGAAGCCATGGTTTTCGCCCATGC-3′ F93A-for: 5′-CGGGAATTCATGGTTGCCGCCCATGCTCAATGGAA-3′. These oligonucleotides and their reverse complement primer pairs were used in each reaction. Each mutagenesis was verified by DNA sequencing. Subsequently, new recombinant baculovirus were generated using the Bac-to-Bac system (Invitrogen), followed by the production of the mutant proteins in insect cells as previously described (*36*). Wild type and mutant protein expression levels were determined by Western blot analysis (data not shown). Kinetic analysis of the mutants with pNP and 4-MU was carried out as described above.

RESULTS

Characterization of Human Recombinant UGT1A Isoforms with p-Nitrophenol (pNP) and 4-Methylumbelliferone (4-MU). A main objective of this study was to characterize and compare the glucuronidating activities of eight human recombinant UGTs toward two model phenol compounds, pNP, a simple planar aromatic phenol containing a single ring, and 4-MU, which contains two rings (for structural comparisons, see Figure 2). The initial experiments were carried out to identify the UGT isoform(s) and photoaffinity probes that were most effective for photoaffinity labeling experiments. The level of expressed protein was evaluated by Western blot using commercially available anti-His and anti-UGT1A antibodies. The protein levels were normalized as described previously (*56*). Enriched membrane preparations of the human recombinant UGTs, UGT1A1, 1A3, 1A4, and 1A6−1A10, expressed as His-tag proteins in baculovirus infected Sf9 insect cells, were characterized with pNP and 4-MU, and the results are presented in Figure 2.

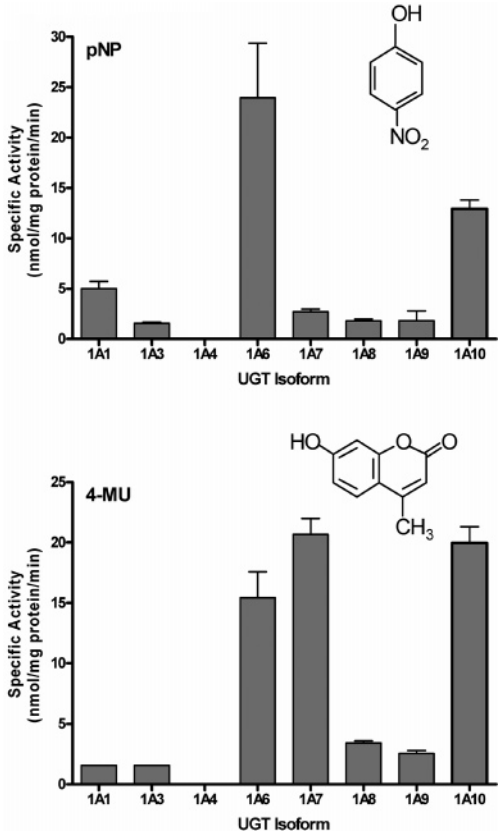

FIGURE 2: Glucuronidation activities of UGT1A1, 1A3, 1A4, 1A6, 1A7, 1A8, 1A9, and 1A10 with 4-nitrophenol (pNP) and 4-methylumbelliferone (4-MU). Glucuronidation activity was measured using membrane fractions of recombinant UGTs expressed as His-tag proteins in baculovirus infected Sf9 insect cells (10 μg). The substrate and cosubstrate (UDP-GlcUA) concentrations were 2 mM and 4 mM, respectively. The phenol substrates were dissolved in DMSO (final concentration 2%), and the reaction was incubated for 20 min. Reactions were stopped by the addition of ethanol, and products were separated by TLC and identified by autoradiography as described in Experimental Procedures. Specific activities are expressed in nmol/mg of protein/min and shown with standard deviations based on (2−6) experiments.

All UGT1A isoforms, with the exception of UGT1A4, glucuronidated both pNP and 4-MU. UGT1A6 was the most active isoform toward pNP, followed by UGT1A10 and 1A1, with activities of approximately 25, 10, and 5 nmol/mg of protein/min, respectively. The pattern of glucuronidation of 4-MU was significantly different from that of pNP. UGT1A6, 1A7, and 1A10 were the most effective isoforms in the

Table 1: Kinetic Constants for 4-Nitrophenol (pNP) and 4-Methylumbelliferone (4-MU) Glucuronidation by Human UGT1A Isoforms[a]

	substrate			
	pNP		4-MU	
isoform	K_m (μM)	V_{max} (nmol/mg of protein/min)	K_m (μM)	V_{max} (nmol/mg of protein/min)
UGT1A1	1034.0	7.1		
UGT1A6	519.1	43.2	237.6	26.8
UGT1A7	150.8	3.2	92.4	26.8
UGT1A8	803.0	2.6	76.6	2.9
UGT1A9	49.6	3.5	52.2	2.8
UGT1A10	335.9	14.1	122.6	18.5

[a] Assays were carried out by incubating membrane fractions containing recombinant UGTs (10 μg) with increasing concentrations (shown in the figure) of [^{14}C]pNP or 4-MU with a constant concentration of UDP-GlcUA (4 mM) for 10 min at 37 °C. Reactions were stopped by the addition of ethanol, and products were separated by TLC and identified by autoradiography as described in Experimental Procedures. (Kinetic parameters for UGT1A1 toward 4-MU were not determined due to the low specific activity found during the screening experiments.) The mean of at least two determinations are shown. K_m and V_{max} values were determined using GraphPad Prism 4 software and are the result of duplicate determinations.

glucuronidation of 4-MU, each catalyzing the reaction equally well (15−20 nmol/mg of protein/min). In addition, this substrate was also glucuronidated to a small extent by all the UGT isoforms under investigation with the exception of UGT1A4.

The apparent K_m and V_{max} values for the glucuronidation of pNP by UGT1A1 and 1A6−10 are given in Table 1. The highest affinity toward pNP was seen with UGT1A9 and 1A7, with apparent K_m values of 50 and 150 μM, respectively. The affinities of the other isoforms were much lower, ranging from approximately 300 to 1000 μM. The V_{max} values were highest for UGT1A6, 1A10, and 1A1: 43.2, 14.1, and 7.1 nmol/mg of protein/min, respectively. The V_{max} values for UGT1A7, 1A8, and 1A9 were very similar, ranging from 2.6 to 3.5 nmol/mg of protein/min. Interestingly, pNP glucuronidation by UGT1A10 appears to decrease at higher concentrations suggesting substrate inhibition (Figure 7). This is in agreement with other examples of substrate inhibition of UGTs that have been observed (*57*); however, the mechanism behind this phenomenon has not been elucidated.

Apparent V_{max} and K_m values with 4-MU were evaluated for UGT1A6−10. The kinetic parameters for these data are shown also in Table 1. In general, the K_m values with this substrate were significantly lower than those for pNP. With UGT1A9, 1A8, and 1A7, K_m values were in the range of 50−100 μM, while, with UGT1A10 and 1A6, the values were slightly higher, 123 and 238 μM, respectively.

Evaluation of the Azido-benzoic Acid Derivatives as Potential Substrates and/or Inhibitors of UGT1A Isoforms. Novel photoreactive azido-containing benzoic acid derivatives were developed and synthesized for the identification of the binding site of UGTs (Figure 1). Attempts to synthesize a direct pNP azido derivative (4-azidophenol) were only marginally successful, due to the fact that the final product was highly unstable and, therefore, unsuitable for enzymatic assays or photoaffinity experiments. The introduction of a carboxyl function into the aromatic ring stabilized the compound, allowing for the synthesis of six different azidobenzoic acid derivatives. The first series of compounds contain the azido group ortho, meta, and para to the carboxyl group. The final three compounds contain an additional nitro, chloro, or hydroxyl group on the ring.

Table 2: Glucuronidation of Azidobenzoic Acid Derivatives by Membrane Fractions of Recombinant UGT1A Isoforms[a]

	substrate			
UGT isoform	4-AzBA	3-AzBA	3-AzCBA	4-AzHBA
	enzymatic activity			
UGT1A6	- -	- -	0.51*	- -
UGT1A7	- -	- -	0.43*	- -
UGT1A9	0.64	- -	0.44	- -
UGT1A10	1.08*	0.14*	0.46	0.57

[a] Glucuronidation of azidobenzoic acid derivatives was measured using enriched membrane fractions prepared from recombinant UGTs expressed as His-tag proteins in baculovirus infected Sf9 insect cells. Substrate concentrations are 200 μM and 500 μM (indicated with an asterisk (*)). The concentration of [^{14}C]UDP-GlcUA was 4 mM. Phenolic substrates were dissolved in DMSO (final concentration 2%). Assays were carried out as described under Experimental Procedures. Enzymatic activity values are expressed in nmol/mg of protein/min and are the result of duplicate determinations. 2-AzNBA and 2-AzBA were not substrates of any of the UGT isoforms tested and are consequently not listed in the table. - -: No activity.

All of the azidobenzoic acid derivatives were characterized as substrates and/or inhibitors of the eight available UGT1A isoforms (Table 2). UGT1A1, 1A3, 1A4, and 1A8 were inactive toward all six azidobenzoic acid derivatives, and no UGT isoform had activity toward 2-AzNBA or 2-AzBA, both of which have the azido group in the ortho position relative to the carboxyl function. UGT1A10 glucuronidated the remaining compounds with varying activity. UGT1A9 glucuronidated both 4-AzBA and 3-AzCBA, while UGT1A6 and 1A7 glucuronidated only 3-AzCBA. Additional analyses of the inhibitory potency and kinetic parameters in the absence of irradiation were carried out with 2-AzNBA, 4-AzBA, 3-AzCBA, and 4-AzHBA (data not shown). All compounds were found to be effective inhibitors of pNP glucuronidation by UGT1A10, and detailed structure−function relationship studies for UGT1A10 with these four compounds are being carried out and will be the topic of separate studies.

Based on these results, detailed kinetic analysis of UGT1A10 activity toward 4-AzHBA (at concentrations of 100 μM to 4 mM) were carried out, and a low apparent K_m (138 μM) and a V_{max} of 0.5 nmol/mg of protein/min were found (data not shown), indicating that UGT1A10 has high affinity for 4-AzHBA. To further establish the utility of 4-AzHBA as a specifically targeted probe for the phenol binding site, experiments examining inhibition of pNP glucuronidation by 4-AzHBA were carried out. The apparent IC_{50} value was approximately 39 μM (Figure 3). These data demonstrate that 4-AzHBA, in addition to being a substrate, also serves as an inhibitor of pNP glucuronidation by UGT1A10, suggesting that it can bind directly in the pNP active site, competing or interfering with pNP binding. These experiments confirmed the suitability of this compound as a photoaffinity probe for the phenol binding site of this UGT. Therefore, UGT1A10 and 4-AzHBA were selected for our first photoaffinity experiments described below.

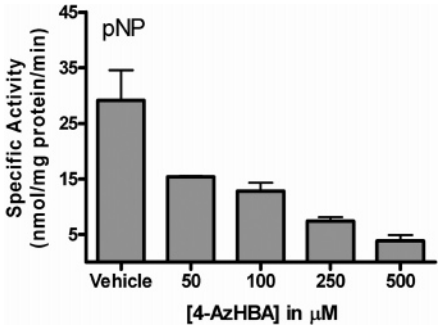

FIGURE 3: Inhibition of UGT1A10 glucuronidation of 4-nitrophenol (pNP) by 4-azido-2-hydroxybenzoic acid (4-AzHBA). Membrane fractions containing 10 μg of UGT1A10 were incubated with increasing concentrations (as shown in the figure) of 4-AzHBA for 2 min, followed by the measurement of [^{14}C]pNP (1mM) glucuronidation. Reactions were stopped by the addition of ethanol, and products were separated by TLC and identified by autoradiography as described in Experimental Procedures. 4-AzHBA was dissolved in DMSO (final concentration 2%). The IC_{50} value was determined using GraphPad Prism 4 software. The graphical fit of the data (mean ± SD of 4−6 determinations) is shown.

Purification of Recombinant UGT1A10. The availability of His-tagged recombinant proteins allowed for the preparation of sufficient amounts of homogeneous UGTs for the photolabeled proteins to be sequenced by LC−MS/MS. The His-tag at the C-terminal end of recombinant UGT1A10 allowed purification using Immobilized Metal Affinity Chromatography (IMAC) on a nickel-charged His Hi-trap column. Figure 4A shows the result of SDS-PAGE analysis of purified UGT1A10 stained with Coomassie blue, while Figure 4B shows the result of Western blot analysis of the purified UGT1A10 using a pan-UGT1A antibody. The multiple bands shown by SDS-PAGE and immunoblot are the result of differing levels of glycosylation, as their molecular mass can be altered by endoglycosidase H treatment (data not shown).

Photoaffinity Labeling of Membrane-Associated and Purified UGT1A10 with 4-Azido-2-hydroxybenzoic Acid (4-AzHBA). For identification of the putative phenol binding site, 4-AzHBA was used as a photoaffinity probe. It is postulated that, upon photoactivation, the azido group of the photoaffinity probe yields a nitrene as a reactive intermediate that covalently binds to amino acids in the vicinity of the probe (*58*). Optimal conditions for photoaffinity labeling with 4-AzHBA, such as the wavelength and time of irradiation and concentration of the photoaffinity probe, were evaluated using UGT1A10 membrane fractions (data not shown). Since the photoprobe was not radioactive, the effectiveness of the photolabeling conditions was evaluated by measuring the ability of the 4-AzHBA photolabeled UGT1A10 membranes to glucuronidate pNP. The photoreactivity of the azido group was established by investigation of the effectiveness of UV irradiation at different wavelengths. This compound presented a strong UV absorbance at 254 nm, and irradiation for 90 s produced optimal photoincorporation, with covalent binding being totally dependent on UV irradiation. Therefore, these conditions were used in all 4-AzHBA labeling experiments. UGT membranes were found to be photolabeled with 4-AzHBA in a concentration-dependent manner, and optimal photoincorporation was achieved at a concentration of 500 μM. Preincubation with various phenol derivatives protected UGT1A10 from photoincorporation of 4-AzHBA in a concentration-dependent manner. All of these data strongly imply that this probe fulfills all the requirements for an effective photoaffinity probe, such as UV dependence, probe concentration dependence, and inhibition of labeling by structurally related compounds. Once the optimal conditions for photoaffinity labeling in membrane fractions were established, purified UGT1A10 protein was labeled with 4-AzHBA for LC/MS sequencing.

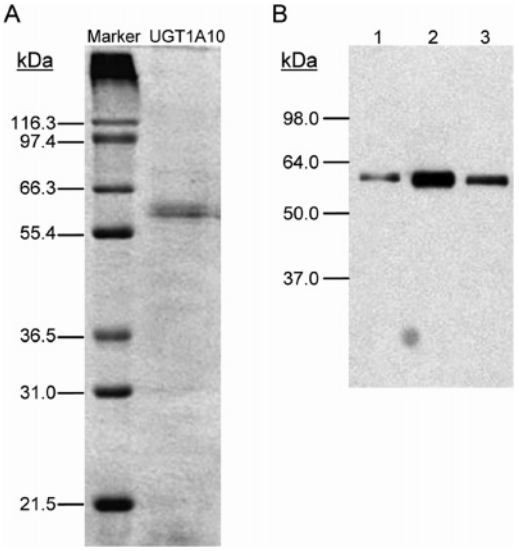

FIGURE 4: Purification of His-tagged recombinant UGT1A10 by immobilized metal affinity chromatography (IMAC). Recombinant UGT1A10 carrying six histidine residues (His-tag) at the C-terminal end expressed in baculovirus-infected insect cells was solubilized and subjected to affinity purification by IMAC using a nickel-loaded column as described in Experimental Procedures. Fractions were analyzed by SDS-PAGE and Western blot. (A) Coomassie blue staining of SDS-PAGE of affinity-purified UGT1A10. About 1 μg of purified recombinant UGT1A10 was loaded on the gel, and proteins were visualized using Coomassie Blue dye. (B) Identification of purified recombinant UGT1A10 by Western blot using anti-UGT1A antibody. Lane 1, 2, and 3: UGT1A10 eluted in 300 mM imidazole fraction 1, 2, and 3, respectively.

Molecular Mass Analysis of Photolabeled UGT1A10 by MALDI-TOF. Tryptic peptide lysates were applied directly to a MALDI spot-plate, followed by time-of-flight analysis of the individual peptides. Figure 5 shows a spectrum obtained for 4-AzHBA-labeled UGT1A10. To identify photolabeled peptides, a neutral ion mass loss of 154 for 4-AzHBA (based on the loss of two nitrogens when the probe is photolyzed) was used. Among the ions identified in the spectrum were two peaks of interest located at 1394 *m*/*z* and 1548 *m*/*z*. These ions are consistent with what would be seen if the polypeptide (amino acids 89−99) formed by tryptic cleavage at the amide bonds following Arg^{88} and Lys^{99} (EFMVFAHAQWK), which appears as a 1394 *m*/*z* peak, was photo-cross-linked with one molecule of 4-AzHBA (1394 + 154). Under the conditions used, neither were other potential adducts detected in the cross-linked samples nor were any adducts detected in the non-crosslinked UGT1A10 control digest.

Identification of 4-AzHBA-Photolabeled Amino Acid Residues by LC−MS/MS. Figure 6 shows the collision-induced dissociation mass spectrum of the 4-AzHBA-photolabeled peptide (amino acids 89−99; 1548 *m*/*z*) that was identified using MALDI-TOF (*41*). The fragmentation pattern with major peaks assigned is shown in Figure 6. All ion fragments

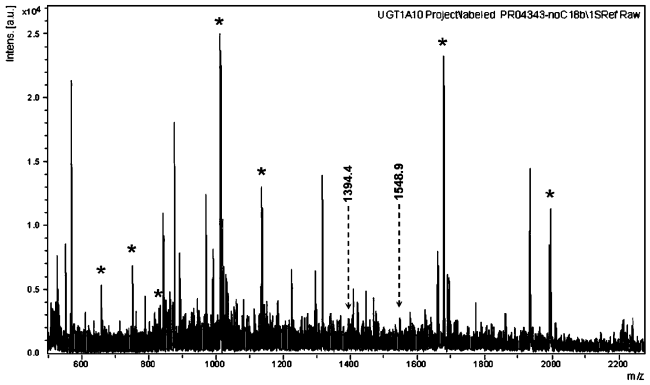

FIGURE 5: MALDI-TOF identification of the amino acid sequence, EFMVFAHAQWK (residues 89−98), as the potential site for 4-azido-2-hydroxybenzoic acid (4-AzHBA) binding in UGT1A10. Tryptic peptide lysate of 4-AzHBA-photolabeled UGT1A10 was applied directly to a MALDI spot-plate, followed by time-of-flight analysis of the individual peptides. Among the ions identified in the spectrum were two peaks of interest located at 1394 *m*/*z* and 1548 *m*/*z*. The amino acid sequence, EFMVFAHAQWK (residues 89−98), was deduced from this spectrum to be the site of attachment of 4-AzHBA.

containing the 4-AzHBA-modified amino acid will have a mass shift of 154 Da.

In the b-ion series, all fragments from b5 (*m*/*z* 808.3) through b9 (*m*/*z* 1215.5) were identified and found to incorporate 4-AzHBA. Thus, the site of incorporation must be within b1−5 (Glu^{89}-Phe^{93}). In the y series, only unmodified fragments were found from y3 (*m*/*z* 461.3) through y6 (*m*/*z* 740.4), again suggesting that the site of incorporation must be within Glu^{89}-Phe^{93}. Both modified and unmodified b4 ions are observed at *m*/*z* 507.2 and 661.2, and in the y series, both modified and unmodified y8 C-terminal fragments are observed at *m*/*z* 986.5 and 1140.5, respectively, suggesting that more than one amino acid in this region could be labeled by 4-AzHBA. No ions consistent with Glu^{89} or Met^{91} being labeled were identified. All these data suggest a high probability that Phe^{90}, Val^{92}, and/or Phe^{93} are the residues labeled with 4-AzHBA.

Site-Directed Mutagenesis. The photoaffinity labeling experiments followed by LC−MS/MS sequencing indicated that Phe^{90} and Phe^{93}, localized in the N-terminal end of UGT1A10, were probable targets of 4-AzHBA and were very likely to be involved in the binding of other simple planar aromatic phenols. The motif FxxF is conserved in four UGT1A isoforms, 1A7−1A10. Therefore, the role of Phe^{90} and Phe^{93} in phenol recognition was evaluated by site-directed mutagenesis. Two recombinant UGT1A10 mutants, F90A and F93A, were constructed by replacing the wild-type amino acid residues Phe^{90} and Phe^{93} with Ala.

Analysis of the glucuronidation activity of the UGT1A10 mutants toward pNP showed a complete loss of activity for the F90A mutant (Figure 7), and toward 4-MU this mutant showed severely impaired activity with a decrease in enzymatic activity (V_{max}) of 82% (Figure 8). Although activity was decreased toward 4-MU, there was no large change in the K_m value (wt: 122 μM; F90A: 151 μM).

The change of Phe^{93} to Ala produced an enzyme with increased catalytic activity toward pNP (125%) but decreased activity toward 4-MU (42%). The affinity of the F93A mutant for 4-MU was decreased 2-fold. However, in the case

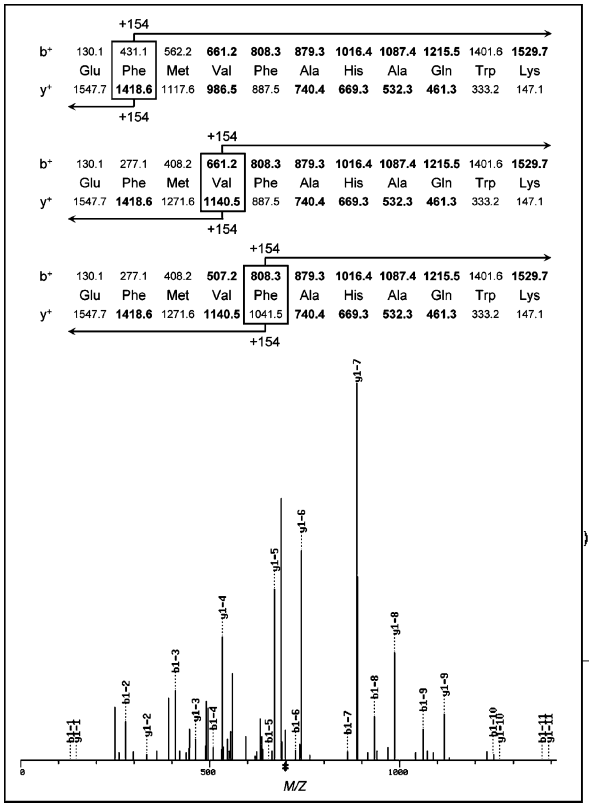

FIGURE 6: LC−MS/MS identification of Phe^{90}, Val^{92}, and Phe^{93} as potential sites for 4-azido-2-hydroxybenzoic acid (4-AzHBA) binding in UGT1A10. Tryptic peptide lysate of 4-AzHBA-photolabeled UGT1A10 was applied to an LCQ Deca MS/MS instrument, and MS/MS ion series for the 1548 *m*/*z* peptide identified by MALDI were determined. At the top of the figure, the predicted charge/mass ratio of N-terminal ions (b-ions) and C-terminal ions (y-ions) are shown above and below the sequence, respectively. Observed *m*/*z* values are in bold. The horizontal arrows show which *m*/*z* values have a mass of 154 Da added to them (see Results). The b- and y-series ions that were detected in this analysis are illustrated in the spectra scan below.

of pNP glucuronidation, the K_m increased more than 10-fold, and under the experimental conditions used, saturation of the reaction was not reached.

DISCUSSION

Our laboratory has originated studies on the localization of UGT active sites by combining photoaffinity labeling with enzymatic digestion, mass spectrometric peptide mapping, and site-directed mutagenesis. The recent development of human recombinant UGTs containing a C-terminal His-tag expressed in baculovirus-infected Sf9 insect cells has resulted in the availability of high levels of expressed proteins that are post-transcriptionally modified by glycosylation and easily purified to homogeneity by IMAC (*36*). Using these purified recombinant proteins, we have attempted to localize the phenol binding site of human UGT1A10. We used the photolabile probe 4-AzHBA to label purified UGT1A10.

After photoaffinity labeling and proteolytic digestion of the conjugated protein, MALDI and LC−MS/MS analysis was used to localize the site of attachment of the photoprobe to the phenol binding site of UGT1A10. In experiments using 4-AzHBA as the photoaffinity probe, MALDI analysis of the peptide fragments of labeled UGT1A10 suggested the

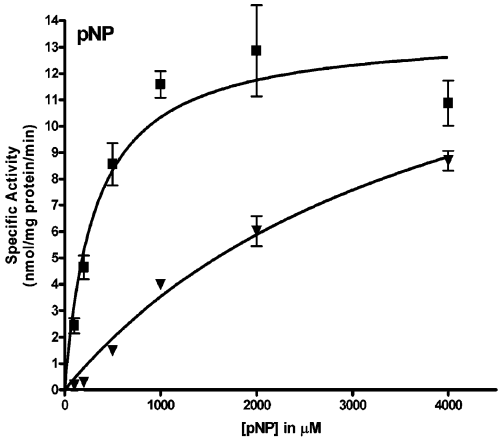

UGT Isoform	K_m (μM)	Vmax (nmol/mg protein/min)	Vmax/Km (μl/mg protein/min)
1A10	380 ± 80	14.33 ± 0.8	37.7
F90A	--	--	--
F93A	3950 ± 930	17.97 ± 2.7	4.5

FIGURE 7: Kinetic constants for 4-nitrophenol (pNP) glucuronidation by recombinant wild-type UGT1A10 (■) and the F90A (▲) and F93A (▼) mutants. Assays were carried out by incubating membrane fractions containing recombinant UGT1A10 and its F to A mutants (10 μg) with increasing concentrations (shown in the figure) of pNP at a constant concentration of [^{14}C]UDP-GlcUA (4 mM) for 10 min at 37 °C. Reactions were stopped by the addition of ethanol and products were separated by TLC and identified by autoradiography as described in Experimental Procedures. Curve fits and kinetic constants were determined using GraphPad Prism 4 software. The graphical fits of the data from each of the analyses with each substrate (mean ± SD of 4−6 determinations) are shown.

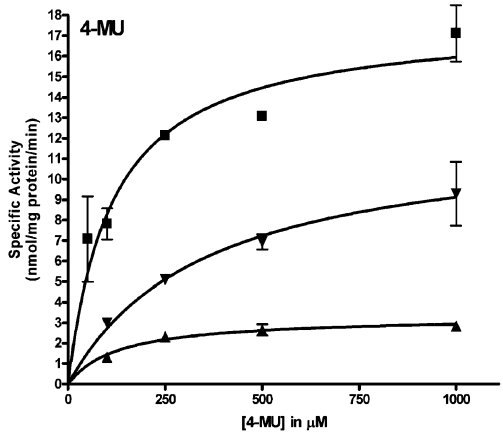

UGT Isoform	K_m (μM)	Vmax (nmol/mg protein/min)	Vmax/Km (μl/mg protein/min)
1A10	122 ± 22.4	18.48 ± 0.9	151.5
F90A	151 ± 26.3	3.38 ± 0.2	22.4
F93A	294 ± 90.3	10.77 ± 1.3	36.6

FIGURE 8: Kinetic constants for 4-methylumbelliferone (4-MU) glucuronidation by recombinant wild-type UGT1A10 (■) and the F90A (▲) and F93A (▼) mutants. Assays were carried out by incubating membrane fractions containing recombinant UGT1A10 and its F to A mutants (10 μg) with increasing concentrations (shown in the figure) of 4-MU at a constant concentration of [^{14}C]-UDP-GlcUA (4 mM) for 10 min at 37 °C. Reactions were stopped by the addition of ethanol, and products were separated by TLC and identified by autoradiography as described in Experimental Procedures. Curve fits and kinetic constants were determined using GraphPad Prism 4 software. The graphical fits of the data from each of the analyses with each substrate (mean ± SD of 4−6 determinations) are shown.

peptide EFMVFAHAQWK (residues 89−99), which is formed by tryptic cleavage of the bonds following Arg^{88} and Lys^{99}, as being the only fragment conjugated with the probe. As the next step, LC−MS/MS analysis of this peptide fragment identified the specific amino acid motif, Phe^{90}-Met^{91}-Val^{92}-Phe^{93}, as the site of 4-AzHBA labeling. The data presented in Figure 6 can be interpreted as indicating that the probe was not bound to a single specific amino acid but was equally likely to be attached to Phe^{90}, Val^{92}, or Phe^{93}.

In the UGT1A10 binding site created by Phe^{90}-Met^{91}-Val^{92}-Phe^{93}, the Phe residues, which have a neutral aromatic side chain, could associate with the phenolic ring of the substrate by hydrophobic aromatic ring stacking interactions. Moreover, both Phe residues were highly conserved in UGT1A7−1A10 (Figure 9). Therefore, as a first step, the significance of these two Phe residues was investigated by site-directed mutagenesis to convert each of these Phe residues to Ala. Alanine has only a short, single carbon side chain; therefore, this mutation greatly reduces the hydrophobicity and eliminates any potential ring stacking interactions. Both the F90A and F93A mutants were successfully expressed as His-tag proteins in the baculovirus infected Sf9 cells, with similar protein expression levels as those of wild-type UGT1A10. The kinetic parameters of the two mutants were then evaluated using two phenolic substrates, pNP and 4-MU, and the results were compared to those of the wild-type enzyme.

Apparent K_m and V_{max} values were affected in both mutants as compared to wild-type; however, the effects of the F90A and F93A mutations were significantly different and strongly dependent on the type of phenol substrate used in glucuronidation assays. As shown in Figures 7 and 8, wild-type UGT1A10 had no preference for pNP or 4-MU as a substrate. However, F90A demonstrated severely impaired glucuronidation activity toward both pNP and 4-MU, with 100% and 82% decreases in V_{max}, respectively, as compared to wild-type UGT1A10.

In the case of the F93A mutant, the V_{max} values obtained for both substrates were almost identical to that of wild-type UGT1A10. In contrast, K_m values for the two mutants appear to depend on the substrate being analyzed. It is clear from the results presented in Figures 7 and 8 that these Phe to Ala substitutions greatly increased the K_m values for pNP but not 4-MU. The K_m values for 4-MU were not markedly affected by the decrease in hydrophobicity at either position.

Mutation of Phe^{90} totally abolished the affinity of UGT1A10 toward pNP, and mutation of Phe^{93} significantly decreased the affinity toward this substrate and affected the K_m. Based on these results, we suggest that the removal of the phenol ring of the Phe residues was the principle determinant of the lack of affinity and the 10-fold increases in the K_m for pNP, with F90A and F93A, respectively, but had minimal effect on the affinity toward 4-MU. It is apparent that both these Phe residues play an important role in the function of this enzyme; however, the specific function of each residue varies. We postulate that Phe^{93} plays a major role in determining the affinity of the enzyme toward various phenolic substrates, resulting in differentiation between single and double ring compounds. On the other hand, Phe^{90} is proposed to be responsible for the level of glucuronidation activity toward both substrates, resulting in the observed impaired

```
UGT1A1   65 SLYIRDGAFYTLKTYPVPFQREDVKESFVSLGHNVFEN--DSFLQRVIKT  112
UGT1A6   64 NLLLKESKYYTRKIYPVPYDQEELKNRYQSFGNNHFAE--RSFLTAPQTE  111
UGT1A7   63 SWQLGRSLNCTVKTYSTSYTLEDQDREFMVFADARWTAPLRSAFSLLTSS  112
UGT1A8   63 SWQLGKSLNCTVKTYSTSYTLEDLDREFMDFADAQWKAQVRSLFSLFLSS  112
UGT1A9   63 SWQLGRSLNCTVKTYSTSYTLEDLDREFKAFAHAQWKAQVRSIYSLLMGS  112
UGT1A10  63 SWQLERSLNCTVKTYSTSYTLEDQNREFMVFAHAQWKAQAQSIFSLLMSS  112
```

FIGURE 9: Amino acid sequence alignment of UGT1A1, 1A6, 1A7, 1A8, 1A9, and 1A10. A sequence alignment of these isoforms from amino acid 63/65 to 111/112 (localized within the N-terminal end of the enzymes) are shown. Six UGT1A isoforms are included for comparison, and the FxxF motifs are indicated. The putative simple phenol binding motif identified in UGT1A6 and a similar motif in UGT1A1 are also shown. Numbers related to the amino acid sequences are based on information deposited in GenBank (UGT1A1: AF180372; UGT1A6: AF014112; UGT1A7: U39570; UGT1A8: U42604; UGT1A9: AF056188; UGT1A10: U39550).

activity following mutation of this residue. The substrate-dependent effects of F90A and F93A on the enzyme activity and affinity observed in the present study (Figures 7 and 8) support a distinct mode of binding and/or catalysis depending on the substrate involved (i.e., 4-MU or pNP). It will be interesting to develop these studies with other UGT1A10 substrates in order to investigate whether the same or different amino acids are involved.

The present studies have focused on the role of these two Phe residues; however, we do not exclude the possibility that other amino acids could also be involved in the binding of phenolic substrates. For example, sequence analysis of UGT1A10 by LC−MS/MS also indicates that Val^{92} might be involved in the cross-linking process (Figure 6). Interestingly, although comparative analysis of the alignment of the amino acid sequences of UGT1A7−1A10 showed that Phe^{90} and Phe^{93} are present in all these isoforms (Figure 9), Val^{92} is only seen in UGT1A7 and 1A10, which have been identified in our studies as isoforms that glucuronidate 4-MU with the highest activity (Figure 2). Information confirming the role of phenylalanines and valine in phenol binding has been provided by the analysis of the coumarin binding site of P450 2A6 (*59*). The X-ray crystal structure was reported for this P450 isoform including crystallization with the substrate coumarin in the active site. In this model, several Phe residues (Phe107, Phe111, Phe118, Phe209, and Phe480) packed together to form the upper surface of the active site cavity. The presence of an FxxxxxVF motif (amino acids 111−118) is extremely relevant to our photoaffinity data for the phenol binding site of UGT1A10 (FxVF).

Sequence alignment also shows that UGT1A6, another phenol specific UGT isoform that has one of the highest activities toward these compounds, does not contain the Phe-Met-Val-Phe peptide motif; however, it does contain a Phe residue that corresponds to Phe^{93} and a Tyr, which only varies from Phe by the addition of a hydroxyl group to the aromatic side chain, that corresponds to Phe^{90} in UGT1A10 (Figure 9). Our previous studies on the photoaffinity labeling of human recombinant UGT1A6 with AzMC resulted in the successful covalent binding of this probe to amino acids in the phenol binding site of this isoform (*28*). In those studies, the putative simple phenol motif was postulated to be YxxxKxxPxP (residues 72−81) based on amino acid alignment of UGT1A6 with several enzymes with activity toward phenols (*28*).

Interestingly, a recent study has shown that mutating Thr^{73} led to total inactivation of both UGT1A7 and UGT1A10, possibly due to the alteration of the phosphorylation state of the enzymes (*41*). This residue is highly conserved (Figure 9), is located within the putative YxxTKxxPxP phenol motif (residues 72−81) that we previously postulated for UGT1A6, and is near the FMVF peptide motif (residues 90−93) identified in the primary sequence of UGT1A10 by photoaffinity labeling in the present study. It is therefore possible that, because of its location within the hypothetical aglycon binding site, the Thr^{73} is essential to maintain the aglycon binding site integrity and enzymatic activity. The availability of homogeneous UGT1A6 and 1A10 protein and two phenol-based probes (4-AzHBA and AzMC) will allow for the rigorous identification of the significance of the two potential phenol binding motifs. Comparative photoaffinity labeling experiments with these two isoforms and 4-AzHBA and identification of the role of Val^{92} in phenol binding are presently under investigation in our laboratory.

Recent studies from the laboratory of Dr. Belanger have reported the isolation of a mutant clone of human UGT1A10 with a mutation occurring at position 211, where Thr^{211} replaced the wild-type Ile^{211} (*42*). Substrate specificity investigations of this mutant showed that all detectable activity toward major UGT1A10 substrates, including phenols, was lost. The authors postulated that this residue is essential for UGT1A10 catalytic activity. This Ile is highly conserved in the majority of UGTs from both the 1A and 2B families and is localized far from the region of highest amino acid sequence variability, which we hypothesize to be the substrate binding region. We did not observe any binding of our probe in this region; however, this is an interesting observation that needs to be investigated further.

Although no reliable information explaining the broad substrate specificity of UGTs is available, two major possibilities can be discussed. It can be hypothesized that (1) one large promiscuous binding site is present or that (2) the catalytic mechanism and substrate specificity of UGTs are determined by the microenvironment formed by a highly variable region of N-terminal amino acid residues composed of multiple amino acid motifs specific for each substrate category. Photoaffinity labeling is currently the only technique available to address this question. Specifically, photolabeling enzymes with multiple probes related to the principle substrates can be applied to the identification of specific binding motifs, including target amino acids. It should be emphasized that although kinetic investigations can provide some basic information on the character of the binding site (number of active sites, etc.), only photoaffinity labeling combined with mass spectrometry sequencing can unambiguously identify the target amino acids.

In summary, this very powerful proteomics approach to the identification of UGT phenol binding sites can be effectively used for the identification of binding sites for

other UGT substrates, as well as for its cosubstrate, UDP-GlcUA. It is widely recognized that UGT binding sites accept a variety of structurally unrelated compounds, and similar promiscuity has been identified for a variety of other drug metabolizing enzymes and nuclear receptors. The identification of the architecture of these binding sites is one of the most challenging problems of structure−function relationship studies. It is anticipated that this photoaffinity labeling strategy can be used for the identification of amino acid motifs of UGTs as well as other drug metabolizing enzymes, nuclear receptors, and transporters.

ACKNOWLEDGMENT

We thank Johanna Mosorin, Sanna Sistonen, and Anna Gallus-Zawada for their excellent technical assistance and greatly appreciate the help of Joanna M. Little in the editing of the manuscript.

REFERENCES

1. Mackenzie, P. I., and Owens, I. S. (1984) Cleavage of nascent UDP-glucuronosyltransferase from rat liver by dog pancreatic microsomes, *Biochem. Biophys. Res. Commun. 122*, 1441−1449.
2. Ouzzine, M., Magdalou, J., Burchell, B., and Fournel-Gigleux, S. (1999) Expression of a functionally active human hepatic UDP-glucuronosyltransferase (UGT1A6) lacking the N-terminal signal sequence in the endoplasmic reticulum, *FEBS Lett. 454*, 187−91.
3. Ouzzine, M., Magdalou, J., Burchell, B., and Fournel-Gigleux, S. (1999) An internal signal sequence mediates the targeting and retention of the human UDP-glucuronosyltransferase 1A6 to the endoplasmic reticulum, *J. Biol. Chem. 274*, 31401−31409.
4. Meech, R., and Mackenzie, P. I. (1998) Determinants of UDP glucuronosyltransferase membrane association and residency in the endoplasmic reticulum, *Arch. Biochem. Biophys. 356*, 77−85.
5. Mackenzie, P. I. (1986) Rat liver UDP-glucuronosyltransferase. Sequence and expression of a cDNA encoding a phenobarbital -inducible form, *J. Biol. Chem. 261*, 6119−6125.
6. Mackenzie, P. I. (1987) Rat liver UDP-glucuronosyltransferase. Identification of cDNAs encoding two enzymes which glucuronidate testosterone, dihydrotestosterone, and b-estradiol, *J. Biol. Chem. 262*, 9744−9749.
7. Radominska-Pandya, A., Ouzzine, M., Fournel-Gigleux, S., and Magdalou, J. (2005) Structure of UDP-glucuronosyltransferases in membranes, *Methods Ezymol.* In press.
8. Dutton, G. J. (1980) *Glucuronidation of Drugs and Other Compounds*, CRC Press Inc., Boca Raton, FL.
9. Radominska-Pandya, A., Czernik, P. J., Little, J. M., Battaglia, E., and Mackenzie, P. I. (1999) Structural and functional studies of UDP-glucuronosyltransferases, *Drug Metab. Rev. 31*, 817−99.
10. Senay, C., Jedlitschky, G., Terrier, N., Burchell, B., Magdalou, J., and Fournel-Gigleux, S. (2002) The importance of cysteine 126 in the human liver UDP-glucuronsyltransferase UGT1A6, *Biochim. Biophys. Acta 1597*, 90−96.
11. Mackenzie, P. I. (1990) Expression of chimeric cDNAs in cell culture defines a region of UDP-glucuronosyltransferase involved in substrate selection, *J. Biol. Chem. 265*, 3432−3435.
12. Ouzzine, M., Antonio, L., Burchell, B., Netter, P., Fournel-Gigleux, S., and Magdalou, J. (2000) Importance of histidine residues for the function of the human liver UDP-glucuronosyltransferase UGT1A6: evidence for the catalytic role of histidine 370, *Mol. Pharmacol. 58*, 1609−1615.
13. Senay, C., Ouzzine, M., Battaglia, E., Pless, D., Cano, V., Burchell, B., Radominska, A., Magdalou, J., and Fournel-Gigleux, S. (1997) Arginine 52 and histidine 54 located in a conserved amino-terminal hydrophobic region (LX2-R52-G−H54-X3-V-L) are important amino acids for the functional and structural integrity of the human liver UDP-glucuronosyltransferase UGT1*6, *Mol. Pharmacol. 51*, 406−13.
14. Coffman, B. L., Kearney, W. R., Goldsmith, S., Knosp, B. M., and Tephly, T. R. (2003) Opioids bind to the amino acids 84 to 118 of UDP-glucuronosyltransferase UGT2B7, *Mol. Pharmacol. 63*, 283−8.
15. Moehs, C. P., Allen, P. V., Friedman, M., and Belknap, W. R. (1997) Cloning and expression of solanidine UDP-glucose glucosyltransferase from potato, *Plant J. 11*, 227−236.
16. Coffman, B. L., Kearney, W. R., Green, M. D., Lowery, R. G., and Tephly, T. R. (2001) Analysis of opiod binding to UDP-glucuronosyltransferase 2B7 fusion proteins using nuclear magnetic resonance spectroscopy, *Mol. Pharmacol. 59*, 1464−1469.
17. Iwano, H., Yokota, H., Ohgiya, S., Yotumoto, N., and Yuasa, A. (1997) A critical amino acid residue, asp446, in UDP-glucuronosyltransferase, *Biochem. J. 325*, 587−591.
18. Iwano, H., Yokota, H., Ohgiya, S., and Yuasa, A. (1999) The significance of amino acid residue Asp446 for enzymatic stability of rat UDP-glucuronosyltransferase UGT1A6, *Arch. Biochem. Biophys. 363*, 116−20.
19. Barbier, O., Girard, C., Breton, R., Belanger, A., and Hum, D. W. (2000) N-glycosylation and residue 96 are involved in the functional properties of UDP-glucuronosyltransferase enzymes, *Biochemistry 39*, 11540−52.
20. Coffman, B. L., King, C. D., Rios, G. R., and Tephly, T. R. (1998) The glucuronidation of opioids, other xenobiotics, and androgens by human UGT2B7Y(268) and UGT2B7H(268), *Drug Metab. Dispos. 26*, 73−77.
21. Dorman, G., and Pestwich, G. D. (2000) Using photolabile ligands in drug discovery and development, *Trends Biotechnol. 18*, 64−77.
22. Chen, G., Battaglia, E., Senay, C., Falany, C. N., and Radominska-Pandya, A. (1999) Photoaffinity labeling probe for the substrate binding site of human phenol sulfotransferase (SULT1A1): 7-azido-4-methylcoumarin, *Protein Sci. 8*, 2151−7.
23. Radominska, A., Drake, R. R., Zhu, X., Veronese, M. E., Little, J. M., Nowell, S., McManus, M. E., Lester, R., and Falany, C. N. (1996) Photoaffinity labeling of human recombinant sulfotransferases with 2-azidoadenosine 3′,5′-[5′-32P]bisphosphate, *J. Biol. Chem. 271*, 3195−9.
24. Chen, G., and Radominska-Pandya, A. (2000) Direct photoaffinity labeling of cellular retinoic acid-binding protein I (CRABP-I) with all-trans-retinoic acid: identification of amino acids in the ligand binding site, *Biochemistry 39*, 12568−74.
25. Radominska-Pandya, A., Chen, G., Samokyszyn, V. M., Little, J. M., Gall, W. E., Zawada, G., Terrier, N., Magdalou, J., and Czernik, P. (2001) Application of photoaffinity labeling with [(3)H] all trans- and 9-cis-retinoic acids for characterization of cellular retinoic acid−binding proteins I and II, *Protein Sci. 10*, 200−11.
26. Radominska-Pandya, A., Chen, G., Czernik, P. J., Little, J. M., Samokyszyn, V. M., Carter, C. A., and Nowak, G. (2000) Direct interaction of all-trans-retinoic acid with protein kinase C (PKC). Implications for PKC signaling and cancer therapy, *J. Biol. Chem. 275*, 22324−30.
27. Radominska-Pandya, A., and Chen, G. (2002) Photoaffinity labeling of human retinoid X receptor beta (RXRbeta) with 9-cis-retinoic acid: identification of phytanic acid, docosahexaenoic acid, and lithocholic acid as ligands for RXRbeta, *Biochemistry 41*, 4883−90.
28. Senay, C., Battaglia, E., Chen, G., Breton, R., Fournel-Gigleux, S., Magdalou, J., and Radominska-Pandya, A. (1999) Photoaffinity labeling of the aglycon binding site of the recombinant human liver UDP-glucuronosyltransferase UGT1A6 with 7-azido-4-methylcoumarin, *Arch. Biochem. Biophys. 368*, 75−84.
29. Little, J. M., Lester, R., Kuipers, F., Vonk, R., Mackenzie, P. I., Drake, R. R., Frame, L., and Radominska-Pandya, A. (1999) Variability of human hepatic UDP-glucuronosyltransferase activity, *Acta Biochim. Pol. 46*, 351−63.
30. Little, J. M., and Radominska, A. (1997) Application of photoaffinity labeling with [11,12-3H]all-trans-retinoic acid to characterization of rat liver microsomal UDP-glucuronosyltransferase(s) with activity toward retinoic acid, *Biochem. Biophys. Res. Commun. 230*, 497−500.
31. Battaglia, E., Nowell, S., Drake, R. R., Magdalou, J., Fournel-Gigleux, S., Senay, C., and Radominska, A. (1997) Photoaffinity labeling studies of the human recombinant UDP-glucuronosyltransferase, UGT1*6, with 5-azido-UDP-glucuronic acid, *Drug Metab. Dispos. 25*, 406−11.
32. Radominska, A., Paul, P., Treat, S., Towbin, H., Pratt, C., Little, J., Magdalou, J., Lester, R., and Drake, R. (1994) Photoaffinity

labeling for evaluation of uridinyl analogues as specific inhibitors of rat liver microsomal UDP-glucuronosyltransferases, *Biochim. Biophys. Acta 1205*, 336−45.

33. Pillot, T., Ouzzine, M., Fournel-Gigleux, S., Lafaurie, C., Tebbi, D., Treat, S., Radominska, A., Lester, R., Siest, G., and Magdalou, J. (1993) Determination of the human liver UDP-glucuronosyltransferase 2B4 domains involved in the binding of UDP-glucuronic acid using photoaffinity labeling of fusion proteins, *Biochem. Biophys. Res. Commun. 197*, 785−91.
34. Pillot, T., Ouzzine, M., Fournel-Gigleux, S., Lafaurie, C., Radominska, A., Lester, R., Drake, R., Treat, S., Siest, G., and Magdalou, J. (1993) Purification and characterization of a catalytically active human liver UDP-glucuronosyltransferase expressed as a fusion protein in *E. coli*, *Biochem. Biophys. Res. Commun. 196*, 473−9.
35. Drake, R. R., Zimniak, P., Haley, B. E., Lester, R., Elbein, A. D., and Radominska, A. (1991) Synthesis and characterization of 5-azido-UDP-glucuronic acid. A new photoaffinity probe for UDP-glucuronic acid-utilizing proteins, *J. Biol. Chem. 266*, 23257−60.
36. Kurkela, M., Garcia-Horsman, J. A., Luukkanen, L., Morsky, S., Taskinen, J., Baumann, M., Kostiainen, R., Hirvonen, J., and Finel, M. (2003) Expression and characterization of recombinant human UDP-glucuronosyltransferases (UGTs). UGT1A9 is more resistant to detergent inhibition than other UGTs and was purified as an active dimeric enzyme, *J. Biol. Chem. 278*, 3536−44.
37. Mojarrabi, B., Butler, R., and Mackenzie, P. I. (1996) cDNA cloning and characterization of the human UDP glucuronosyltransferase, UGT1A3, *Biochem. Biophys. Res. Commun. 225*, 785−790.
38. Strassburg, C. P., Oldhaffer, K., Manns, M. P., and Tukey, R. H. (1997) Differential expression of the UGT1A locus in human liver, biliary, and gastric tissue: Identification of UGT1A7 and UGT1A10 transcripts in extrahepatic tissue, *Mol. Pharmacol. 52*, 212−220.
39. Strassburg, C. P., Manns, M. P., and Tukey, R. H. (1998) Expression of the UDP-glucuronosyltransferase 1A locus in human colon. Identification and characterization of the novel extrahepatic UGT1A8, *J. Biol. Chem. 273*, 8719−26.
40. Zheng, Z., Fang, J.-L., and Lazarus, P. (2002) glucuronidation: an important mechanism for detoxification of benzo[*a*]pyrene metabolites in aerodigestive tract tissues, *Drug Metab. Dispos. 30*, 397−403.
41. Basu, N. K., Kovarova, M., Garza, A., Kubota, S., Saha, T., Mitra, P. S., Banerjee, R., Rivera, J., and Owens, I. S. (2005) Phosphorylation of a UGT-glucuronosyltransferase regulates substrate specificity, *Proc. Natl. Acad. Sci. U.S.A. 102*, 6285−6290.
42. Martineau, I., Tchernof, A., and Belanger, A. (2004) Amino acid residue ILE211 is essential for the enzymatic activity of human UDP-glucuronosyltransferase 1A10 (UGT1A10), *Drug Metab. Dispos. 32*, 455−459.
43. Uchaipichat, V., Mackenzie, P. I., Guo, X. H., Gardner-Stephen, D., Galetin, A., Houston, J. B., and Miners, J. O. (2004) Human udp-glucuronosyltransferases: isoform selectivity and kinetics of 4-methylumbelliferone and 1-naphthol glucuronidation, effects of organic solvents, and inhibition by diclofenac and probenecid, *Drug Metab. Dispos. 32*, 413−23.
44. Basu, N. K., Kubota, S., Meselhy, M. R., Ciotti, M., Chowdhury, B., Hartori, M., and Owens, I. S. (2004) Gastrointestinally distributed UDP-glucuronosyltransferase 1A10, which metabolizes estrogens and nonsteridal antiinflammatory drugs, depends on phosphorylation, *J. Biol. Chem. 279*, 28320−28329.
45. Lewinsky, R. H., Smith, P. A., and Mackenzie, P. I. (2005) Glucuronidation of bioflavonoids by human UGT1A10: structure−function relationships, *Xenobiotica 35*, 117−129.
46. Little, J. M., Kurkela, M., Sonka, J., Jantti, S., Ketola, R., Bratton, S., Finel, M., and Radominska-Pandya, A. (2004) Glucuronidation of oxidized fatty acids and prostaglandins B1 and E2 by human hepatic and recombinant UDP-glucuronosyltransferases, *J. Lipid Res. 45*, 1694−703.
47. Elahi, A., Bendaly, J., Zheng, Z., Muscat, J. E., Richie, J. P., Jr., Schantz, S. P., and Lazarus, P. (2003) Detection of UGT1A10 polymorphisms and their association with orolaryngeal carcinoma risk, *Cancer 98*, 872−80.
48. Mojarrabi, B., and Mackenzie, P. I. (1997) The human UDP glucuronosyltransferase, UGT1A10, glucuronidates mycophenolic acid, *Biochem. Biophys. Res. Commun. 238*, 775−778.
49. Cheng, Z., Radominska-Pandya, A., and Tephly, T. R. (1999) Studies on the substrate specificity of human intestinal UDP-lucuronosyltransferases 1A8 and 1A10, *Drug Metab. Dispos. 27*, 1165−70.
50. Tukey, R. H., and Strassburg, C. P. (2000) Human UDP-glucuronosyltransferases: metabolism, expression and disease, *Annu. Rev. Pharmacol. Toxicol. 40*, 581−616.
51. Nowell, S. A., Massengill, J. S., Williams, S., Radominska-Pandya, A., Tephly, T. R., Cheng, Z., Strassburg, C. P., Tukey, R. H., MacLeod, S. L., Lang, N. P., and Kadlubar, F. F. (1999) Glucuronidation of 2-hydroxyamino-1-methyl-6-phenylimidazo-[4,5-b]pyridine by human microsomal UDP-glucuronosyltransferases: identification of specific UGT1A family isoforms involved, *Carcinogenesis 20*, 1107−14.
52. Kuuranne, T., Kurkela, M., Thevis, M., Schanzer, W., Finel, M., and Kostiainen, R. (2003) Glucuronidation of anabolic androgenic steroids by recombinant human UDP-glucuronosyltransferases, *Drug Metab. Dispos. 31*, 1117−24.
53. Zhang, P., Graminski, G. F., and Armstrong, R. N. (1991) Are the histidine residues of glutathione S-transferase important in catalysis? An assessment by ^{13}C NMR spectroscopy and site-specific mutagenesis, *J. Biol. Chem. 266*, 19475−19479.
54. Suckau, D., Resemann, A., Schuerenberg, M., Hufnage, P., Franzen, J., and Holle, A. (2003) A novel MALDI LIFT-TOF/TOF mass spectrometer for proteomics, *Anal. Bioanal. Chem. 376*, 952−965.
55. Perkins, D. N., Pappin, D. J., Creasy, D. M., and Cottrell, J. S. (1999) Probability-based protein identification by searching sequence database using mass spectrometry data, *Electrophoresis 20*, 3551−3567.
56. Kurkela, M., Hirvonen, J., Kostiainen, R., and Finel, M. (2004) The interactions between the N-terminal and C-terminal domains of the human UDP-glucuronosyltransferases are partly isoform-specific, and may involve both monomers, *Biochem. Pharmacol. 68*, 2443−50.
57. Lepine, J., Bernard, O., Plante, M., Têtu, B., Pelletier, G., Labrie, F., and Bêlanger, A. (2004) Specificity and regioselectivity of the conjugation of estradiol, estrone, and their catecholestrogen and methoxyestrogen metabolites by human uridine diphospho-glucuronosyltransferases expressed in endometrium, *J. Clin. Endocrinol. Metab. 89*, 5222−5232.
58. Knorre, D. G., and Godovikova, T. S. (1998) Photoaffinity labeling as an approach to study supramolecular nucleoprotein complexes, *FEBS Lett. 433*, 9−14.
59. Yano, J. K., Hsu, M. H., Griffin, K. J., Stout, C. D., and Johnson, E. F. (2005) Structures of human microsomal cytochrome P450 2A6 complexed with coumarin and methoxsalen, *Nat. Struct. Mol. Biol. 12*, 822−3.

BI0519001